A Concentrated Aqueous Solution of Chromium Dichloride for Chromium Metal Electrodeposition

Kazuhiko Matsumoto,[a],* Jingyuan Zhang,[a] Nozomi Yoneda,[a] Koma Numata,[b] Kazuki Okuno,[b] Rika Hagiwara,[a]

[a]Graduate School of Energy Science, Kyoto University, Sakyo-ku, Kyoto 606-8501, Japan

[b]Sumitomo Electric Industries Ltd., 1-1-3 Koya-kita, Itami, Hyogo 664-0016, Japan

Corresponding Author

* E-mail: k-matsumoto@energy.kyoto-u.ac.jp

ABSTRACT

Concentrated electrolytes have been found to play host to stellar phenomena previously unachievable in solutions at diluted or moderate concentrations. In an attempt to explore the possible utility of concentrated electrolytes in electroplating, this study reports the electrodeposition of Cr metal using a concentrated aqueous solution of Cr(II) (4.0 mol kg^{-1}) without additives. Target aqueous $CrCl_2$ solutions are characterized by UV-visible spectroscopic and ionic conductivity measurements. The influence of concentration, current density, and agitation on Cr metal deposition is discussed on the basis of cyclic voltammetry, galvanostatic electrolysis, X-ray diffraction, and scanning electron microscopy. Here, electrolysis of the concentrated electrolyte at medium current densities (20 mA cm^{-2}) under agitation is found to engender dense metallic α-Cr deposits with high adhesivity to the substrate. The results further show that increasing the current density to expedite the deposition process promotes the involvement of an impurity phase and deposition of the δ-Cr phase.

INTRODUCTION

Concentrated electrolytes have been acclaimed as a gateway to new chemistries that play host to new phenomena previously unachievable by solutions at diluted or moderate concentrations. In spite of these prospects, the high concentrations embodied by these solutions generally engender high viscosities and consequently low ionic conductivities – properties that render them unsuitable for electrolyte inquests which generally put precedence on high ionic conductivities. Nonetheless, recent works on concentrated electrolytes have unveiled an assortment of functionalities that promise novel application avenues, such as in rechargeable battery systems. In these electrochemical systems, concentrated electrolytes have been found to engender safety and performance improvements arising from the formation of stable solid-electrolyte interphases coupled with their ability to extend the breakup voltages, irrespective of solvents employed (i.e., aqueous and non-aqueous solutions).[1-7] The absence (or significant decrease) of solvent molecules not coordinated to metal ions entails unique electrochemical reactions that cannot be visualized at moderate concentrations due to the strong interactions between solvents and metal ions that lead to changes in electronic states. These providential electrochemical reactions have also found utility in metal electrodeposition, where concentrated electrolytes have been reported to expedite the plating of Li,[8-11] Na,[12-14] K,[15-16], and Zn[17-19] metals by previous works.

Electrodeposition is an important process that allows the deployment of a swath of metallic elements in industrial operations ranging from bulk electrolysis to surface coating.[20-22] In one of the applications of electrodeposition, Cr metal obtained from aqueous solutions is often coated onto metal materials to enhance their corrosion resistance, surface hardness, and even aesthetics. However, the efficacy of this process (so-called chrome plating) is typically encumbered by concurrent H_2 gas evolution and the accompanying low current efficiencies.[23-24] Additionally, the

highly toxic nature of some common electrolytic solutions, such as those containing Cr(VI) species, presents hurdles to practical applications.[25] As such, Cr(III) species are seen as safer alternatives, becoming subjects of focus in numerous Cr electrodeposition studies.[23-24, 26-31] Even so, these aqueous solutions often require delicate and complicated adjustments of electrolytic conditions along with the application of additives to improve their efficacies. Notwithstanding, the crystallinity and quality of the deposits derived from Cr(III) species still tend to be significantly lower than those obtained from Cr(VI) species even after optimization processes.

Besides the Cr(III) and Cr(VI) species highlighted above, the electrodeposition of Cr metal can also be achieved with aqueous Cr(II) solutions, but their utility is relatively underexplored.[23] Although Cr(II) is susceptible to oxidation in air, it can sustain electrolysis using a low total charge if appropriately handled under an O_2-free atmosphere. Considering the expedited electroplating observed in previous studies, the present work explores the electrodeposition of Cr metal from a concentrated aqueous solution of $CrCl_2$ without any additives. Herein, aqueous $CrCl_2$ solutions of varying concentrations are characterized through UV-visible (UV-Vis) spectroscopy and ionic conductivity measurements. Further, cyclic voltammetry and galvanostatic electrolysis are employed to elucidate the influence of concentration, current density, and agitation on the electrochemical behavior of selected electrolytic solutions. The structure and morphology of the Cr metal deposited are finally investigated using optical microscopy, X-ray diffraction (XRD), and scanning electron microscopy (SEM).

METHODS

General procedure and materials. All the air-sensitive materials including $CrCl_2$ and its solutions were handled under an Ar atmosphere in a glove box or a glove bag. Anhydrous $CrCl_2$

(Sigma-Aldrich, 99.99%) and Cr plate (Nilaco, 99.9%) were used as supplied. Nickel plate (Nilaco, 99%) was treated with hydrochloric acid (10 wt%) for one min prior to use. Distilled water was deoxygenated by passing Ar gas for 20 min. Aqueous $CrCl_2$ solutions at different concentrations were prepared by mixing $CrCl_2$ and the distilled water in a target ratio (1.0, 2.0, or 4.0 mol kg^{-1}). This process is exothermic and careful handling is required.

Electrochemical measurements. Electrochemical properties were evaluated using an HZ-7000 electrochemical measurement system (Hokuto Denko) under an Ar atmosphere. A three-electrode electrolytic cell was used with Ni working (0.5 cm × 0.5 cm) and Cr counter (0.4 cm × 3.0 cm) electrodes. The AgCl/Ag reference electrode with a 3.0 mol dm^{-3} KCl solution (0.208 V vs. standard hydrogen electrode) was separated from the electrolytic solution by porous glass filter. The electrolytic solution was agitated with a stirring bar if necessary.

Analytical methods. Solubility of $CrCl_2$ into water was determined by inductively coupled plasma spectroscopy using a Thermo Fisher Scientific iCAP™ PRO XP ICP-OES. Ionic conductivities were measured using AC impedance with a 3532−80 impedance analyzer (Hioki E.E. Corp.). The samples for the ionic conductivity measurements were sealed in an airtight T-shaped cell equipped with stainless-steel disk electrodes under an atmosphere of dry Ar (see Figure S1 for the schematic of the cell). The cell was set in an SU-241 thermostatic chamber (ESPEC Corp.). The electrode samples were washed with distilled water after electrolysis and dried in the air for analysis. Surface morphology of the cathode after galvanostatic electrolysis was observed by a digital microscope (Keyence VHX-5000) equipped with a VH-ZST object lens. The crystalline phases of electrodeposits were analyzed by a Rigaku SmartLab X-ray diffractometer with Ni-filtered Cu Kα radiation (40 kV and 30 mA) and a Si strip high-speed detector (Rigaku D/teX Ultra 250) at the

scan rate of 5 deg min^{-1}. Cross-sectional images of the electrodeposit and substrate were obtained by a FlexSEM 1000-II scanning electron microscope (Hitachi High-Tech).

RESULTS AND DISCUSSION

Physical properties. The solubility of CrCl$_2$ in water was evaluated using inductively coupled plasma atomic emission spectroscopy (ICP-AES), which determined saturation to occur at the concentration of 4.0 mol kg^{-1} with a corresponding H$_2$O/Cr^{2+} ratio of approximately 14. The saturation at this concentration was further ascertained through visual scrutiny and UV spectroscopic data. A summary of the UV-Vis spectra and ionic conductivity data from selected CrCl$_2$ solutions is provided in Figure 1. The spectra of the CrCl$_2$ solutions (Figure 1a) are marked by large absorption peaks (around 750 nm) that are assigned to Cr(II). The intensity of these peaks is seen to saturate at concentrations slightly above 4.0 mol kg^{-1}, in accord with the solubility results from ICP-AES. Additionally, weak absorption peaks appearing in the 400 to 450 nm range are assigned to Cr(III) species (407 nm for [Cr(OH$_2$)$_6$]$^{3+}$, 430 nm for [Cr(OH$_2$)$_5$Cl]$^{2+}$, and 450 nm for [Cr(OH$_2$)$_4$Cl$_2$]$^+$).[32] Accordingly, CrCl$_2$ concentrations of 1.0, 2.0, and 4.0 mol kg^{-1} were selected to evaluate the temperature dependence of their ionic conductivities, as shown in Figure 1b (see Table S1 for ionic conductivities at different temperatures). In this series, the ionic conductivity of the solutions can be seen to increase when the concentration is increased from 1.0 to 2.0 mol kg^{-1} (where it achieved maximal values) but thereafter decline when the concentration is further increased to 4.0 mol kg^{-1} (1.0, 2.0, and 4.0 mol kg^{-1} solutions deliver 101, 131, and 71.8 mS cm^{-1}, respectively, at 25 °C). The diminished conductivity at high concentrations is ascribed to the increased ion association; typical behavior for electrolytic solutions in this concentration range.[33] Moreover, increasing the concentration results in a non-linear increase in the activation energy
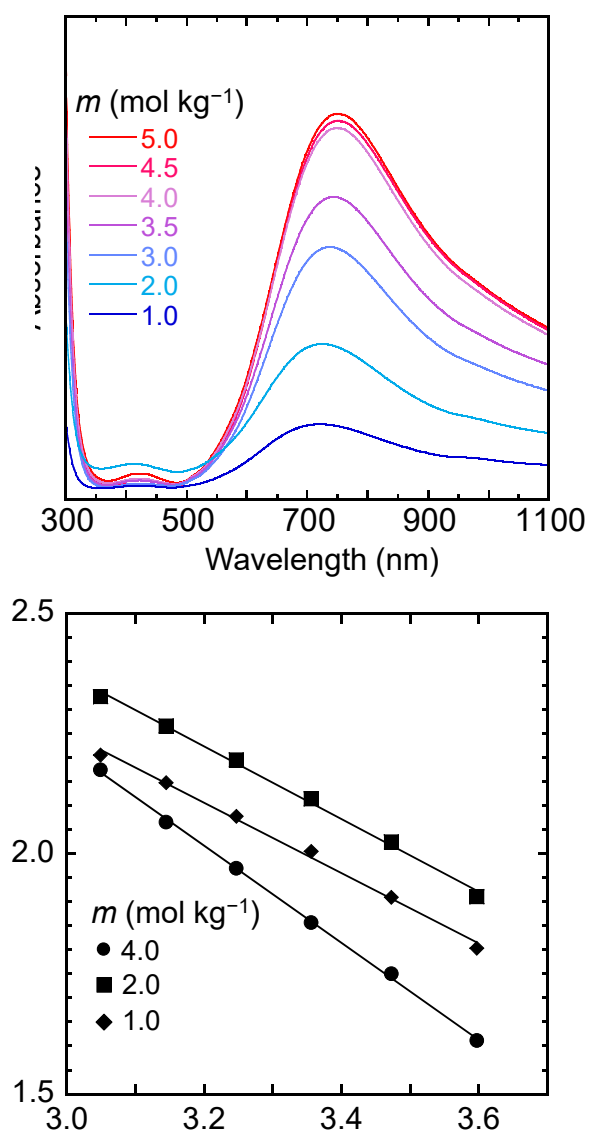
Figure 1 (a) UV-Vis spectra of $CrCl_2$ solutions at varied concentrations. The absorption peaks around 750 nm are assigned to Cr(II). (b) Temperature-dependent ionic conductivity plots of the $CrCl_2$ solutions at different concentrations (E_a = 14.0, 14.5, and 19.3 kJ mol^{-1}).

(E_a) required for ionic conductivity (14.0, 14.5, and 19.3 kJ mol^{-1} for 1.0, 2.0, and 4.0 mol kg^{-1}, respectively), implying that ion diffusion is dominated by ion-ion and ion-dipole interactions.[34] The high ionic conductivities visualized in the present CrCl$_2$ solutions clearly affirm their suitability as electrolytes for Cr metal electrodeposition.

Effects of concentration on the electrochemical behavior and deposit. The electrochemical behavior of the present CrCl$_2$ solutions was investigated, as shown in Figure 2. Cyclic voltammetry (Figure 2a) was performed using a Ni working electrode to investigate the reduction behavior of Cr(II) at the selected concentrations (1.0, 2.0, and 4.0 mol kg^{-1}). Here, the first cathodic waves were observed to commence at around -0.6 V vs. AgCl/Ag regardless of the electrolyte concentration. However, during the shift towards the positive potentials, the second waves were particularly characterized by steeper increases in current density when concentration was increased (-1.2 V vs. AgCl/Ag in the case of 4.0 mol kg^{-1}). Considering the standard redox potential of Cr^{2+}/Cr (-1.13 V vs. AgCl/Ag) and the gas evolution visualized from -0.6 V vs. AgCl/Ag onwards, the first and second waves can be attributed to H$_2$ gas evolution and Cr metal deposition, respectively. Notably, the 4.0 mol kg^{-1} electrolyte exhibits suppressed H$_2$ gas evolution, due to the reduced amounts of free H$_2$O molecules. These observations ratify that Cr metal deposition can be achieved through the electrolysis of highly concentrated Cr(II) solutions, even though the process is accompanied by some degree of H$_2$ gas evolution that is dependent on the electrolysis conditions. Although a Cr metal anode was used in the present experiment, Cr dissolution was not plausible according to our electrochemical analysis (see Figure S2 for details on the anodic behavior of a Cr metal electrode).
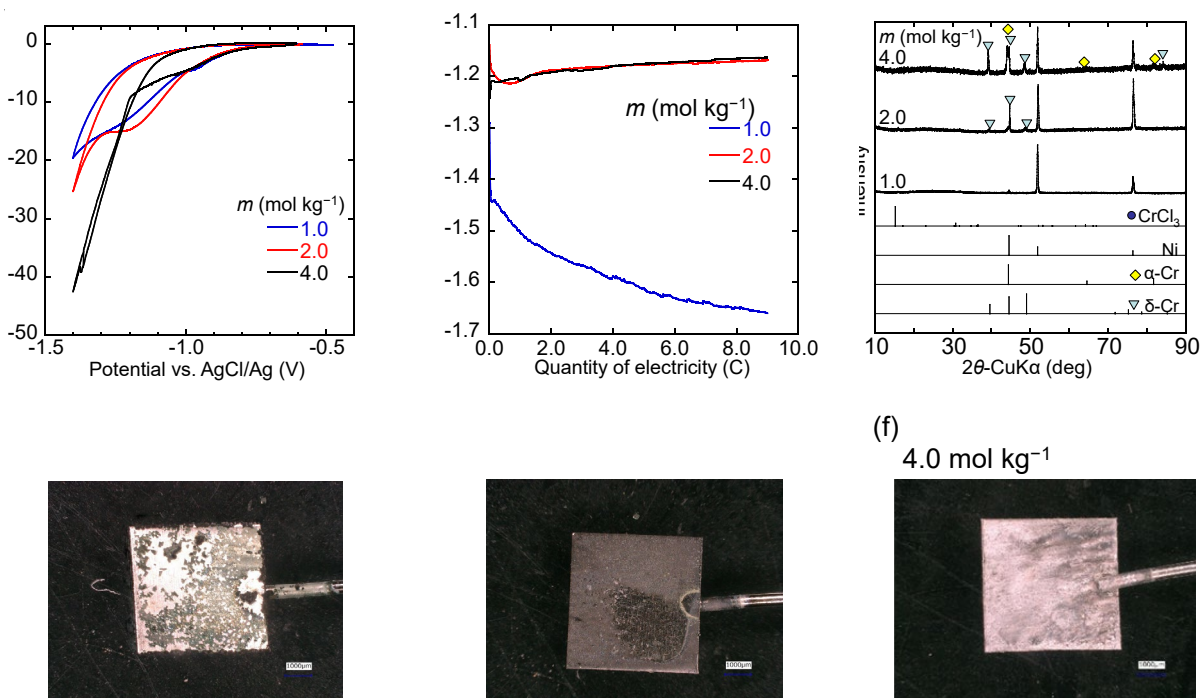
Figure 2 Electrochemical behavior of the 1.0, 2.0, and 4.0 mol kg^{-1} CrCl$_2$ solutions. (a) Cyclic voltammograms of a Ni electrode at a scan rate of 10 mV s^{-1}. (b) Cathode potential during galvanostatic electrolysis at 20 mA cm^{-2} with agitation. Cathode: Ni plate and anode: Cr plate. (c) XRD patterns of the cathodes after galvanostatic electrolysis corresponding to (b). Scan rate: 5 deg min^{-1}. (d−e) Optical microscopic images of the cathodes after galvanostatic electrolysis corresponding to (b).

A probe into the electrochemical data and visual examination of the deposits obtained through the galvanostatic electrolysis of the CrCl$_2$ solutions additionally suggest that Cr metal deposition was enhanced at higher concentrations. Cathode potentials during galvanostatic electrolysis of 2.0 and 4.0 mol kg^{-1} CrCl$_2$ solutions with agitation are close to each other and significantly larger than that of 1.0 mol kg^{-1} CrCl$_2$ solution (Figure 2b). Nevertheless, the deposits from 2.0 and 4.0 mol kg^{-1} CrCl$_2$ solutions have different crystal phases and appearance. X-ray diffraction pattern of the deposit from 1.0 mol kg^{-1} CrCl$_2$ solution does not include any crystalline

material including Cr metal (Figure 2c). On the other hand, δ-Cr is observed for the deposit from 2.0 and 4.0 mol kg^{-1} solutions. Deposition of α-Cr is confirmed for the deposit from 4.0 mol kg^{-1} solution, whereas it is not clear for the deposit from 2.0 mol kg^{-1} solution (see the following section for the difference of α- and δ-phases). This observation suggests that α-Cr is preferably deposited from the solution at high concentrations. By considering the effects of current density on the deposit (see below), the increase of concentration seems to have the same effect as the decrease of current density, which is understandable in terms of the supply of Cr(II) species at the cathode surface. Appearance of the cathodes after galvanostatic electrolysis also changes, depending on the concentration (Figure 2d−f). Metallic surface is observed for the cathode from 4.0 mol kg^{-1} CrCl$_2$ solution, whereas dark non-metallic surface is observed for those from 1.0 and 2.0 mol kg^{-1}. The deposits from 1.0 and 2.0 mol kg^{-1} solutions do not fully cover the substrate. These observations indicate the effectiveness of Cr metal deposition from highly concentrated CrCl$_2$ solution.

Effects of current density on the electrochemical behavior and deposit. For deeper insight into the Cr metal deposition behavior of the CrCl$_2$-saturated solution (4.0 mol kg^{-1}), galvanostatic electrolysis was performed at current densities varying from 5 to 100 mA cm^{-2} with and without applied agitation. All investigations were done using a total charge of 9 C. Figure 3a shows the cathode (Ni substrate; surface area = 0.50 cm^2) potential during galvanostatic electrolysis at 5, 50, and 100 mA cm^{-2}. A plot of the average cathode potentials during electrolysis at 5, 10, 20, 30, 50, and 100 mA cm^{-2} is provided in Figure 3b (for the cathode potential during galvanostatic
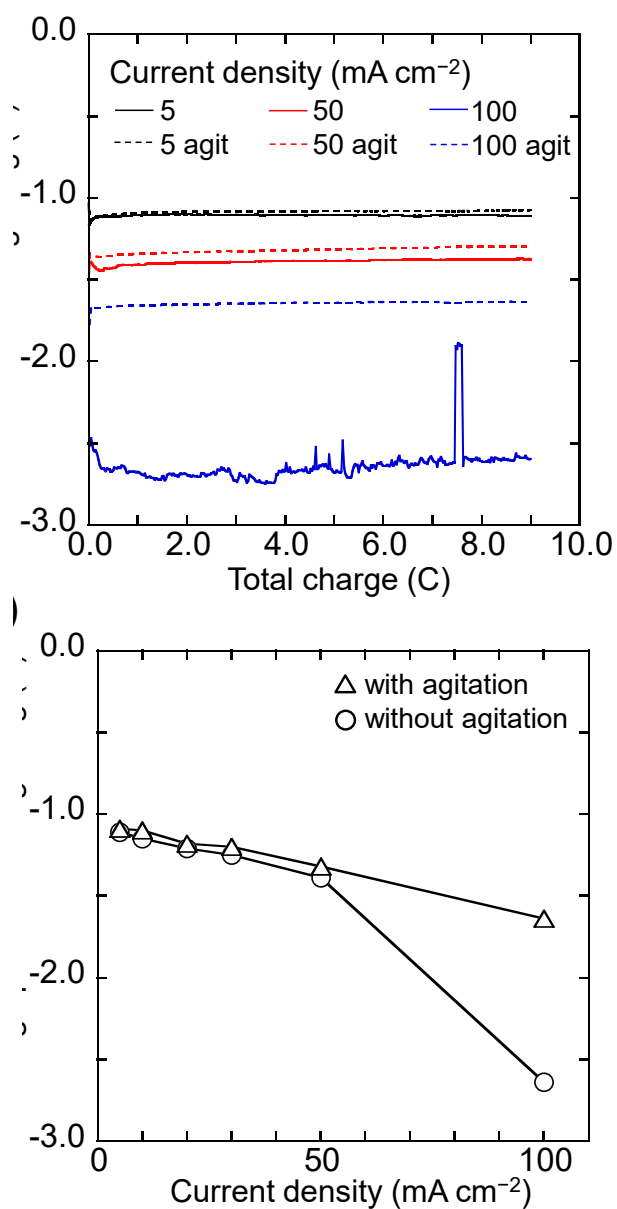
Figure 3 Electrochemical behavior of a Ni cathode (surface area = 0.5 cm^2) in the 4.0 mol kg^{-1} CrCl$_2$ solution during galvanostatic electrolysis with and without applied agitation. Electrolysis time: 60, 30, 15, 10, 6, and 3 min for 5, 10, 20, 30, 50, and 100 mA cm^{-2}, respectively. (a) Correlation between the total charge and cathode potential during electrolysis. (b) Average cathode potentials during electrolysis (see Figure S3 for the correlation between total charge and cathode potential at all the current densities).

electrolysis at all the current densities, see Figure S3). During the galvanostatic electrolysis, the potentials were seen to decrease (larger negative values) with increasing current densities; while agitation was noted to generally provide higher potentials (smaller negative values). Notably, the effect of agitation on the electrode potentials was more prominent at higher current densities, evincing that the supply of Cr(II) was more dominant during the electrode processes at high current densities. The fluctuating cathode potentials observed in some cases are ascribed to the H_2 gas evolution accompanying the process.

Figure 4 summarizes the optical microscopic images, current efficiencies based on the mass increase, crystalline phases identified by XRD, and appearance of the electrodeposits obtained under varied current densities with and without applied agitation. It should be noted that the current efficiencies of some deposits containing Cr(III) species (identified by XRD) could not be accurately evaluated, as will be discussed in a later section. Nonetheless, for the limited cases where accurate estimation was possible, current efficiencies were noted to improve with increasing current densities. Electrolysis without applied agitation formed black and gray deposits on the substrates whereon metallic luster was not visualized. On the other hand, deposits acquired from electrolysis under agitation were characterized by a metallic gloss whose luster increased with decreasing current densities. In fact, the deposits derived at high current densities were black and gray, resembling those obtained without applied agitation. Further, the deposit acquired at 100 mA cm^{-2} was observed to easily peel off the substrate, denoting that increasing the current density aggravates the adhesivity of the deposits. These results suggest that agitation during the supply of Cr(II) from a concentrated electrolyte is essential to the formation of a homogeneous Cr metal film
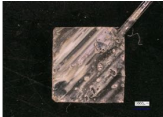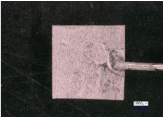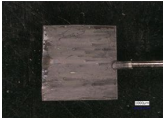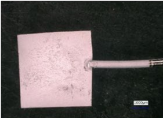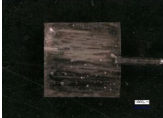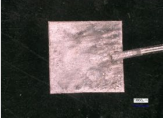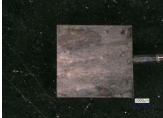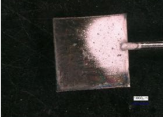
i (mA cm^{-2})	Without agitation		With agitation	
5		(η = 78%) α-Cr, δ-Cr, CrCl$_3$ metallic, black stripes		η = 16% α-Cr metallic
10		(η = 107%) α-Cr, δ-Cr, CrCl$_3$ gray		η = 45% α-Cr metallic
20		(η = 103%) δ-Cr, CrCl$_3$ black		η = 58% α-Cr, δ-Cr metallic
30		(η = 132%) δ-Cr, CrCl$_3$ gray		η = 91% δ-Cr metallic, black
50		(η = 124%) δ-Cr, CrCl$_3$ black		(η = 70%) δ-Cr, CrCl$_3$ black, partly metallic
100		(η = 103%) δ-Cr, CrCl$_3$ black, gray, exfoliative		(η = 124%) δ-Cr, CrCl$_3$ black, gray

Figure 4 Visual summary of the optical microscopic images, current efficiency (η), crystalline phases identified by XRD, and appearance of the cathodic electrodeposits obtained by galvanostatic electrolysis of the 4.0 mol kg^{-1} CrCl$_2$ solution at varied current densities (i). The current efficiencies were estimated on the basis of the mass increase. Accurate estimation was not possible when deposition of Cr(III) species was indicated by XRD (η values are in parentheses in such cases). The length of the substrate's sides is 5 mm. The corresponding XRD patterns are shown in Figure S4.

that is adhesive to the substrate.

The cathodes obtained after galvanostatic electrolysis at current densities varying from 5 to 100 mA cm^{-2} in the CrCl$_2$-saturated electrolyte were subjected to XRD analysis (Figure S4). The patterns show that the deposits comprise two Cr metal polymorphs (α-Cr and δ-Cr) alongside CrCl$_3$ (or its related compounds). According to previous works and the potential-pH diagram,[26, 35-36] H$_2$ gas evolution at the cathode during electrolysis engenders a local increase in pH that facilitates the formation of Cr(III) species. The resulting species is possibly Cr$_2$O$_3$, Cr(OH)$_4^-$, or Cl-containing oxide/hydroxide. The present diffraction patterns display minor peaks, around $2\theta =$ 15.3°, and 31.8°, that can be ascribed to CrCl$_3$. However, it should be pointed out that these diffraction patterns can also be a result of the involvement of OH, which can substitute the Cl in the Cr(III) compounds to produce similar peaks in close proximity to the diffraction angles observed. Chemical formation of Cr(III) from the CrCl$_2$ solution in the absence of oxygen gas was not observed in the present conditions. In any case, these patterns are observed to mostly appear when black or gray deposits are formed, suggesting that these non-lustrous deposits result from the deposition of Cr(III) species. Detailed characterization of this Cr(III) species requires further analysis, which will be performed in our future work. The α-Cr phase manifests the body-centered cubic structure commonly found in Cr metal. The δ-Cr phase with the A-15 type primitive cubic structure is less common but has previously been detected in a deposit obtained from evaporating Cr metal in Ar gas at low pressures or under vacuum.[37-40] The δ-Cr phase has also been attained after annealing electrodeposition products from a CrCl$_3$ methanol solution or as deposits from aqueous CrCl$_3$ solutions containing LiCl.[26, 41] In the present case, agitated electrolysis at 5, 10, and 20 mA cm^{-2} yields α-Cr ($2\theta =$ 44.4°, 64.6°, and 81.7°); whereas δ-Cr ($2\theta =$ 39.6°, 44.5°, 49.0°, 71.8°, 75.2°, and 78.6°) appears in deposits obtained above 20 mA cm^{-2} (both are α- and δ-phases

are deposited at 20 mA cm^{-2}). On the other hand, electrolysis performed without applied agitation produces δ-Cr as the main deposit (α-Cr is obtained only at 5 mA cm^{-2}). These observations indicate that the deposition of δ-Cr occurs due to Cr(II) ion deficiency at the electrode surface and is possibly accompanied by a localized increase in pH, although the latter requires further investigation for clarification.

Cross-sectional SEM images of the cathodes after galvanostatic electrolysis at 5, 20, 50, and 100 mA cm^{-2} with and without applied agitation were obtained as shown in Figure 5. The total charge was maintained at 9 C in all cases. The images indicate that increasing the current density from 5 to 20 mA cm^{-2} under agitation, increases the thickness of the deposits, in consonance with the previous, current efficiency observations (Figure 4: 16% and 58% at 5 and 20 mA cm^{-2}, respectively). Notably, the deposit obtained at 5 mA cm^{-2} does not cover the entire surface of the Ni substrate due to low current efficiency. Further, increasing the current density from 20 to 50 and 100 mA cm^{-2} produces a considerably thick deposit that clearly appears to crack and exfoliate from the substrate, indicating the presence of Cr(III) species alongside Cr metal at high current densities. These observations confirm that medium current densities (20 mA cm^{-2} in this series) provide the smoothest and most adhesive deposit from the saturated CrCl$_2$ solution. XRD analysis additionally corroborates the importance of agitating the solution during electrolysis as a measure against Cr(III) deposition. Moreover, agitation is also found to prevent the deposition of metal films with low adhesivity. Comparing the cathodes at 20 mA cm^{-2} with and without applied agitation, the adverse properties of the Cr(III) species (thick deposits with low adhesivity) formed without applied agitation are clearly discerned.
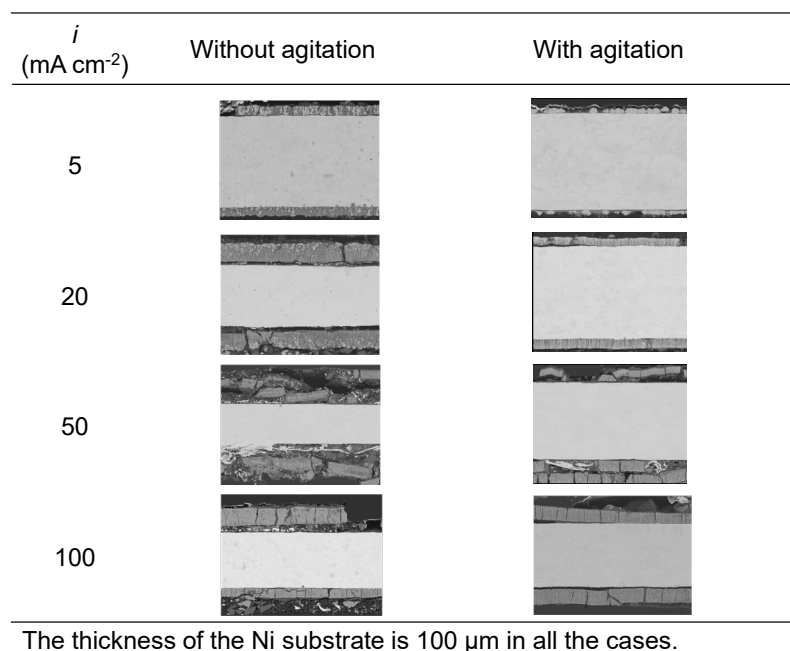
i (mA cm^{-2})	Without agitation	With agitation
5		
20		
50		
100		

The thickness of the Ni substrate is 100 μm in all the cases.

Figure 5 Cross sectional SEM images of the cathodes (Ni substrate) after galvanostatic electrolysis at 5, 20, 50, and 100 mA cm^{-2} without and with agitation.

CONCLUSIONS

Considering the restrictions imposed by the high toxicity of Cr(VI) species, the development of new electrodeposition techniques is vital for the utilization of Cr metal in electroplating. In the search for alternatives, this study evaluated the viability of a concentrated CrCl$_2$ aqueous solution as an electrolytic bath for Cr metal electrodeposition. The saturated electrolyte (4.0 mol kg^{-1}) exhibits suppressed H$_2$ evolution and enhanced Cr metal deposition at the cathode due to the limited amount of free water molecules at high concentrations. Here, electrolysis at medium current densities (20 mA cm^{-2}) under agitation was found to engender the smoothest Cr metal deposits with high adhesivity. Although this study demonstrated the expedience of Cr(II) species in Cr metal electrodeposition, further optimization of electrolytic conditions for higher current efficiency and enhanced adhesivity is still needed for practicality. Future explorations into

substrate pretreatment, ideal electrode configurations, functional additives, and suitable

electrolytic modes are expected to offer possible avenues for efficacy improvements.

ASSOCIATED CONTENT

Supporting Information (PDF)

Supporting Information is available free of charge on the ACS Publications website at DOI: XXXXXXX.

> Additional experimental details, materials, and methods, including schematic of conductivity measurement cell, data for ionic conductivity, electrochemical measurements, and XRD.

AUTHOR INFORMATION

Corresponding Author

E-mail: k-matsumoto@energy.kyoto-u.ac.jp (K.M.).

Notes

The authors declare no competing financial interest.

ORCID

Kazuhiko Matsumoto: 0000-0002-0770-9210

Yoneda Nozomi: 0000-0002-8509-9841

Rika Hagiwara: 0000-0002-7234-3980

REFERENCES

1.   Yamada, Y.; Yamada, A., Review-Superconcentrated Electrolytes for Lithium Batteries. *J. Electrochem. Soc.* **2015,** *162*, A2406-A2423.

2.   Li, M.; Wang, C. S.; Chen, Z. W.; Xu, K.; Lu, J., New Concepts in Electrolytes. *Chem. Rev.* **2020,** *120*, 6783-6819.

3.   Suo, L. M.; Borodin, O.; Gao, T.; Olguin, M.; Ho, J.; Fan, X. L.; Luo, C.; Wang, C. S.; Xu, K., "Water-in-Salt" Electrolyte Enables High-Voltage Aqueous Lithium-Ion Chemistries. *Science* **2015,** *350*, 938-943.

4.   Zhang, H.; Qin, B. S.; Han, J.; Passerini, S., Aqueous/Nonaqueous Hybrid Electrolyte for Sodium-Ion Batteries. *ACS Energy Lett.* **2018,** *3*, 1769-1770.

5.   Yamada, Y.; Usui, K.; Sodeyama, K.; Ko, S.; Tateyama, Y.; Yamada, A., Hydrate-Melt Electrolytes for High-Energy-Density Aqueous Batteries. *Nat. Energy* **2016,** *1*, 16129.

6.   Basile, A.; Hilder, M.; Makhlooghiazad, F.; Pozo-Gonzalo, C.; MacFarlane, D. R.; Howlett, P. C.; Forsyth, M., Ionic Liquids and Organic Ionic Plastic Crystals: Advanced Electrolytes for Safer High Performance Sodium Energy Storage Technologies. *Adv. Energy. Mater.* **2018,** *8*, 1703491.

7.   Matsumoto, K.; Hwang, J.; Kaushik, S.; Chen, C. Y.; Hagiwara, R., Advances in Sodium Secondary Batteries Utilizing Ionic Liquid Electrolytes. *Energ. Environ. Sci.* **2019,** *12*, 3247-3287.

8.   Horstmann, B.; Shi, J. Y.; Amine, R.; Werres, M.; He, X.; Jia, H.; Hausen, F.; Cekic-Laskovic, I.; Wiemers-Meyer, S.; Lopez, J., et al, Strategies Towards Enabling Lithium Metal in Batteries: Interphases and Electrodes. *Energ. Environ. Sci.* **2021,** *14*, 5289-5314.

9.   Nilsson, V.; Kotronia, A.; Lacey, M.; Edstrom, K.; Johansson, P., Highly Concentrated Litfsi-Ec Electrolytes for Lithium Metal Batteries. *ACS Appl Energ Mater* **2020,** *3*, 200-207.

10.   Ugata, Y.; Thomas, M. L.; Mandai, T.; Ueno, K.; Dokko, K.; Watanabe, M., Li-Ion Hopping Conduction in Highly Concentrated Lithium Bis(Fluorosulfonyl)Amide/Dinitrile Liquid Electrolytes. *Phys. Chem. Chem. Phys.* **2019,** *21*, 9759-9768.

11.   Jiang, G. X.; Li, F.; Wang, H. P.; Wu, M. G.; Qi, S. H.; Liu, X. H.; Yang, S. C.; Ma, J. M., Perspective on High-Concentration Electrolytes for Lithium Metal Batteries. *Small Struct* **2021,** *2*, 2000122.

12.   Forsyth, M.; Yoon, H.; Chen, F. F.; Zhu, H. J.; MacFarlane, D. R.; Armand, M.; Howlett, P. C., Novel Na^+ Ion Diffusion Mechanism in Mixed Organic-Inorganic Ionic Liquid Electrolyte Leading to High Na^+ Transference Number and Stable, High Rate Electrochemical Cycling of Sodium Cells. *J. Phys. Chem. C* **2016,** *120*, 4276-4286.

13.   Schafzahl, L.; Hanzu, I.; Wilkening, M.; Freunberger, S. A., An Electrolyte for Reversible Cycling of Sodium Metal and Intercalation Compounds. *ChemSusChem* **2017,** *10*, 401-408.

14.   Lee, J.; Lee, Y.; Lee, J.; Lee, S. M.; Choi, J. H.; Kim, H.; Kwon, M. S.; Kang, K.; Lee, K. T.; Choi, N. S., Ultraconcentrated Sodium Bis(Fluorosulfonyl)Imide-Based Electrolytes for High-Performance Sodium Metal Batteries. *ACS Appl. Mater. Inter.* **2017,** *9*, 3723-3732.

15.   Hosaka, T.; Kubota, K.; Kojima, H.; Komaba, S., Highly Concentrated Electrolyte Solutions for 4 V Class Potassium-Ion Batteries. *Chem. Commun.* **2018,** *54*, 8387-8390.

16.   Yang, F. H.; Hao, J. N.; Long, J.; Liu, S. L.; Zheng, T.; Lie, W.; Chen, J.; Guo, Z. P., Achieving High-Performance Metal Phosphide Anode for Potassium Ion Batteries Via Concentrated Electrolyte Chemistry. *Adv. Energy. Mater.* **2021,** *11*, 2003346.

17.   Chen, C. Y.; Matsumoto, K.; Kubota, K.; Hagiwara, R.; Xu, Q., A Room-Temperature Molten Hydrate Electrolyte for Rechargeable Zinc-Air Batteries. *Adv. Energy. Mater.* **2019,** *9*, 201900196.

18.   Wang, F.; Borodin, O.; Gao, T.; Fan, X. L.; Sun, W.; Han, F. D.; Faraone, A.; Dura, J. A.; Xu, K.; Wang, C. S., Highly Reversible Zinc Metal Anode for Aqueous Batteries. *Nature Mater.* **2018,** *17*, 543-549.

19.   Zhang, C.; Holoubek, J.; Wu, X. Y.; Daniyar, A.; Zhu, L. D.; Chen, C.; Leonard, D. P.; Rodriguez-Perez, I. A.; Jiang, J. X.; Fang, C., et al, A Zncl2 Water-in-Salt Electrolyte for a Reversible Zn Metal Anode. *Chem. Commun.* **2018,** *54*, 14097-14099.

20.   Paunovic, M.; Schlesinger, M., *Fundamentals of Electrochemical Deposition, 2nd Ed.* John Wiley & Sons: Hoboken, 2006.

21.   Djokić, S. S., *Electrodeposition and Surface Finishing: Fundamentals and Applications*. Springer Science: New York, 2014.

22.   Kanani, N., *Electroplating: Basic Principles, Processes and Practice*. Elsevier Science: Oxford, 2004.

23.   Kasper, C., The Deposition of Chromium from Solutions of Chromic and Chromous Salts. *Bur. Stand. J. Res.* **1933,** *11*, 515-526.

24.   Dennis, J. K.; Such, T. E., *Nickel and Chromium Plating, 3rd Ed.* Woodhead Publishing: Cambridge, 1993.

25.   Dayan, A. D.; Paine, A. J., Mechanisms of Chromium Toxicity, Carcinogenicity and Allergenicity: Review of the Literature from 1985 to 2000. *Hum. Exp. Toxicol.* **2001,** *20*, 439-451.

26.   Adachi, K.; Kitada, A.; Fukami, K.; Murase, K., Crystalline Chromium Electroplating with High Current Efficiency Using Chloride Hydrate Melt-Based Trivalent Chromium Baths. *Electrochim. Acta* **2020,** *338*, 135873.

27.   Safonov, V. A.; Vykhodtseva, L. N.; Polukarov, Y. M.; Safonova, O. V.; Smolentsev, G.; Sikora, M.; Eeckhout, S. G.; Glatzel, P., Valence-to-Core X-Ray Emission Spectroscopy Identification of Carbide Compounds in Nanocrystalline Cr Coatings Deposited from Cr(Iii) Electrolytes Containing Organic Substances. *J. Phys. Chem. B* **2006,** *110*, 23192-23196.

28.   Protsenko, V. S.; Danilov, F. I.; Gordiienko, V. O.; Kwon, S. C.; Kim, M.; Lee, J. Y., Electrodeposition of Hard Nanocrystalline Chrome from Aqueous Sulfate Trivalent Chromium Bath. *Thin Solid Films* **2011,** *520*, 380-383.

29.   Song, Y. B.; Chin, D. T., Current Efficiency and Polarization Behavior of Trivalent Chromium Electrodeposition Process. *Electrochim. Acta* **2002,** *48*, 349-356.

30.   Zeng, Z. X.; Sun, Y. L.; Zhang, J. Y., The Electrochemical Reduction Mechanism of Trivalent Chromium in the Presence of Formic Acid. *Electrochem. Commun.* **2009,** *11*, 331-334.

31.   Tu, Z. M.; Yang, Z. L.; Zhang, J. S.; An, M. Z.; Li, W. L., Cathode Polarization in Trivalent Chromium Plating. *Plat. Surf. Finish.* **1993,** *80*, 79-82.

32.   Elving, P. J.; Zemel, B., Absorption in the Ultraviolet and Visible Regions of Chloroaquochromium(Iii) Ions in Acid Media. *J. Am. Chem. Soc.* **1957,** *79*, 1281-1285.

33.   Izutsu, K., *Electrochemistry in Nonaqueous Solutions*. 2nd Revised and Enlarged ed.; Wiley-VCH: 2009.

34.   Yim, C. H.; Abu-Lebdeh, Y. A., Connection between Phase Diagram, Structure and Ion Transport in Liquid, Aqueous Electrolyte Solutions of Lithium Chloride. *J. Electrochem. Soc.* **2018,** *165*, A547-A556.

35.   Beverskog, B.; Puigdomenech, I., Revised Pourbaix Diagrams for Chromium at 25-300 Degrees C. *Corros. Sci.* **1997,** *39*, 43-57.

36.   Surviliene, S.; Nivinskiene, O.; Cesuniene, A.; Selskis, A., Effect of Cr(Iii) Solution Chemistry on Electrodeposition of Chromium. *J. Appl. Electrochem.* **2006,** *36*, 649-654.

37.   Doherty, C. J.; Poate, J. M.; Voorhoeve, R. J. H., Vacuum-Evaporated Films of Chromium with a-15 Structure. *J. Appl. Phys.* **1977,** *48*, 2050-2054.

38.   Nishida, I.; Kimoto, K., Crystal Habit and Crystal-Structure of Fine Chromium Particles - Electron-Microscope and Electron-Diffraction Study of Fine Metallic Particles Prepared by Evaporation in Argon at Low-Pressures (Iii). *Thin Solid Films* **1974,** *23*, 179-189.

39.   Forssell, J.; Persson, B., Growth and Structure of Thin Chromium Films Condensed on Ultra-High Vacuum Cleaved Nacl and Kcl Crystals. *J. Phys. Soc. Jpn.* **1970,** *29*, 1532-&.

40.   Chu, J. P.; Chang, J. W.; Lee, P. Y.; Wu, J. K.; Wang, J. Y., On the Formation of Nonequilibrium A15 Crystal Structure Chromium Thin Films by Sputter Deposition. *Thin Solid Films* **1998,** *312*, 78-85.

41.   Tsuru, T.; Takenaka, I.; Kobayashi, S.; Inui, T., Electrodeposition of Chromium from Chromium(Iii) Chloride Hexahydrate-Methanol Baths. *J. Surf. Finish. Soc. Jpn.* **1977,** *28*, 85-89.

TOC GRAPHICS